Article

Small-Angle Neutron and X-ray Scattering from Amphiphilic Stimuli-Responsive Diamond-Type Bicontinuous Cubic Phase

Borislav Angelov, Angelina Angelova, Vasil M. Garamus, Genevive Lebas, Sylviane Lesieur, Michel Ollivon, Srgio S. Funari, Regine Willumeit, and Patrick Couvreur

J. Am. Chem. Soc., **2007**, 129 (44), 13474-13479• DOI: 10.1021/ja072725+ • Publication Date (Web): 11 October 2007

J|A|C|S
ARTICLES
Published on Web 10/11/2007

Small-Angle Neutron and X-ray Scattering from Amphiphilic Stimuli-Responsive Diamond-Type Bicontinuous Cubic Phase

Borislav Angelov,[†,||] Angelina Angelova,*[,‡,§] Vasil M. Garamus,[||] Geneviève Lebas,[‡,§] Sylviane Lesieur,[‡,§] Michel Ollivon,[‡,§] Sérgio S. Funari,[⊥] Regine Willumeit,[||] and Patrick Couvreur[‡,§]

Contribution from the Institute of Biophysics, Bulgarian Academy of Sciences, BG-1113 Sofia, Bulgaria, CNRS UMR8612 Physico-chimie, Pharmacotechnie, Biopharmacie, Châtenay-Malabry, F-92290 France, Université Paris Sud, Châtenay-Malabry, F-92290 France, Institute of Materials Research, GKSS Research Center, Geesthacht, D-21502 Germany, and HASYLAB c/o DESY, Notkestrasse 85, Hamburg, D-22603 Germany

Received April 19, 2007; Revised Manuscript Received August 23, 2007; E-mail: Angelina.Angelova@u-psud.fr

Abstract: The structural evolution of a diamond-type bicontinuous lipid cubic phase upon application of thermal and chemical (hydration agent) stimuli is investigated by means of small-angle neutron (SANS) and X-ray scattering (SAXS). The soft-matter cubic architecture responds by dramatic swelling (D_{Large} cubic structure) upon incorporation of a hydration-enhancing guest component (octyl glucoside) at low and ambient temperatures, the aqueous channel diameter increasing twice to ~7 nm. D_{Large} appears to be built up from an assembly of cubosomic domains, which may coexist with an amphiphilic lamellae domain at low temperatures. The chemical stimulus concentration can be selected as to tune the hydration of the nanochannels in the D_{Large} phase and its transformation into a D_{Normal} phase at temperatures above the body temperature. Two-dimensional SANS images recorded upon heating scan reveal growth of spontaneously oriented domains of single-crystal cubic nature. Phase separation and squeezing out the guest-hydrating agent from the higher-curvature regions of the amphiphilic bilayer suggest a possible mechanism for the established transformations. The order−order structural transition, cubic D_{Large} − cubic D_{Normal}, is found to be reversible upon cooling. The obtained results put forward a structure-based concept for release of encapsulated guest molecules from stimuli-responsive and self-regulated cubosomic nanocarriers.

Introduction

Spontaneous self-assembly of amphiphiles in aqueous medium may generate ordered complex fluid systems and nanostructures based on liquid crystalline (LC) supramolecular architectures such as lamellar, inverted hexagonal, bicontinuous cubic, sponge, etc.[1−14] Soft-matter bicontinuous cubic mesophases[15−25] (BCP) of nonionic and nontoxic amphiphiles are suitable for design of nanostructured carrier and delivery systems

[†] Bulgarian Academy of Sciences.
[‡] CNRS UMR8612 Physico-chimie, Pharmacotechnie, Biopharmacie.
[§] Université Paris Sud.
[||] Institute of Materials Research, GKSS Research Center.
[⊥] HASYLAB. Dr. Michel Ollivon is deceased.

(1) Lynch, M. L., Spicer P. T., Eds. *Bicontinuous Liquid Crystals*; Surfactant Science Series, Vol.127; Taylor & Francis: Boca Raton, 2005.
(2) Case, F., Alexandridis, P., Eds. *Mesoscale Phenomena in Fluid Systems*; ACS Symposium Series 861; American Chemical Society: Washington DC, 2003.
(3) (a) Whitesides, G. M.; Grzybowski, B. *Science* **2002**, *295*, 2418−2421. (b) Wu, H.; Thalladi, V. R.; Whitesides, S.; Whitesides, G. M. *J. Am. Chem. Soc.* **2002**, *124*, 14495−14502.
(4) (a) Hamley, I. W. *Angew. Chem., Int. Ed.* **2003**, *42*, 1692−1712. (b) Finnefrock, A. C.; Ulrich, R.; Toombes, G. E. S.; Gruner, S. M.; Wiesner, U. *J. Am. Chem. Soc.* **2003**, *125*, 13084−13093.(c) Ellison, L. J.; Michel, D. J.; Barmes, F.; Cleaver, D. J. *Phys. Rev. Lett.* **2006**, *97*, 237801.
(5) (a) Lodge, T. P.; Rasdal, A.; Li, Z.; Hillmyer, M. A. *J. Am. Chem. Soc.* **2005**, *127*, 17608−17609. (b) Park, M. J.; Bang, J.; Harada, T.; Char, K.; Lodge, T. P. *Macromolecules* **2004**, *37*, 9064−9075.
(6) Johnsson, M.; Barauskas, J.; Tiberg, F. *J. Am. Chem. Soc.* **2005**, *127*, 1076−1077.
(7) Nekovee, M.; Coveney, P. V. *J. Am. Chem. Soc.* **2001**, *123*, 12380−12382.
(8) Zeng, X., Ungar, G.; Impèror-Clerk, M. *Nat. Mater.* **2005**, *4*, 562−567.
(9) (a) Hyde, S. T.; Schroder, G. E. *Curr. Opin. Colloid Interface Sci.* **2003**, *8*, 5−14. (b) Ndoni, S.; Vigild, M. E.; Berg, R. H. *J. Am. Chem. Soc.* **2003**, *125*, 13366−13367.
(10) (a) Lapitsky, Y.; Eskuchen, W. J.; Kaler, E. W. *Langmuir* **2006**, *22*, 6375−6379. (b) Petrov, J. G., Angelova, A., Mobius, D. *Langmuir* **1992**, *8*, 206−212.
(11) Spicer, P. T.; Small, W. B.; Lynch, M. L.; Burns, J. L. *J. Nanopart. Res.* **2002**, *4*, 297−311.
(12) (a) Borné, J.; Nylander, T.; Khan, A. *J. Phys. Chem. B* **2002**, *106*, 10492−10500. (b) Barauskas, J.; Misiunas, A.; Gunnarsson, T.; Tiberg, F.; Johnsson, M. *Langmuir* **2006**, 22, 6328−6334.
(13) (a) Yaghmur, A.; de Campo, L.; Sagalowicz, L.; Leser, M. E.; Glatter, O. *Langmuir* **2006**, *22*, 9919−9927. (b) Yaghmur, A.; de Campo, L.; Sagalowicz, L.; Leser, M.; Glatter, O. *Langmuir* **2005**, *21*, 569−577. (c) Bryskhe, K.; Schillen, K.; Olsson, U.; Yaghmur, A.; Glatter, O. *Langmuir* **2005**, *21*, 8597−8600. (d) Leser, M. E.; Sagalowicz, L.; Michel, M.; Watzke, H. J. *Adv. Colloid Interface Sci.* **2006**, *123*−*126*, 125−136.
(14) (a) Paccamiccio, L.; Pisani, M.; Spinozzi, F.; Ferrero, C.; Finet, S.; Mariani, P. *J. Phys. Chem B* **2006**, *110*, 12410−12418. (b) Ropers, M. H.; Stebe, M. J. *Phys. Chem. Chem. Phys.* **2001**, *3*, 4029−4036.
(15) (a) Luzzati, V. *Curr. Opin. Struct. Biol.* **1997**, *7*, 661−668. (b) Luzzati, V. *J. Phys. II* **1995**, *5*, 1649−1669.
(16) (a) Rançon, Y.; Charvolin, J. *J. Phys. Chem.* **1988**, *92*, 2646−2651. (b) Rançon, Y.; Charvolin, J. *J. Phys. Chem.* **1988**, *92*, 6339−6344. (c) Clerc, M. Levelut, A. M., Sadoc, J. F. *J. Phys. II* **1991**, *1*, 1263−1276.
(17) Hyde, S.; Andersson, S.; Larsson, K.; Blum, Z.; Landh, T.; Lidin, S.; Ninham, B. W. *The Language of Shape*; Elsevier Science: New York, 1996.
(18) (a) Larsson, K. *Nature* **1983**, *304*, 664. (b) Hyde, S.T.; Andersson, S.; Ericsson, B.; Larsson, K. *Z. Kristallogr.* **1984**, *168*, 213−219.
(19) Lindblom, G.; Larsson, K.; Johansson, L.; Fontell, K.; Forsen, S. *J. Am. Chem. Soc.* **1979**, *101*, 5465−5470.

10.1021/ja072725+ CCC: $37.00

for pharmaceutical, cosmetics, biotechnology, and food applications.[13,26−31] They could serve for nanoconfinement and encapsulation of active ingredients as well as templates for synthesis of nanomaterials.[32−42] Their high structural stability in excess aqueous medium is a further advantage for biomedical applications.[33c]

The control of the diameter of the nanofluidic aqueous channels that constitute the overall periodic three-dimensional (3D) network architecture[15,17−22] of BCP, is important in the context of encapsulation and release of therapeutic substances from cubosomic nanocarriers.[33a−c] Recently, we found that the inclusion of the hydration-modulating agent octyl glucoside (OG), as a guest component in the self-assembly monoolein (MO)/water system, may serve for tuning of the diameters of the aqueous nanochannels in the diamond-type BCP under excess water conditions.[25a] That study has suggested the need of further structural research on the mechanism of transition and reversibility between swollen and normal-type BCP as a function of the applied stimuli, namely concentration of the nanochannel-hydration enhancing agent and temperature.

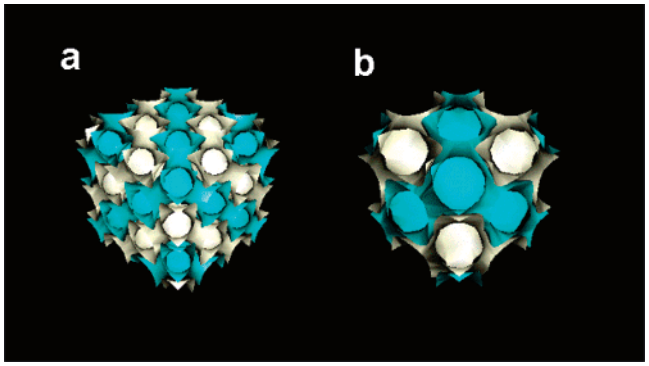

Figure 1. Three-dimensional model presentation of bicontinuous diamond-type cubic nanostructures D_{Normal} (a) and D_{Large} (b). Amphiphilic bilayer decorates a periodic minimal 3D surface of a double-diamond cubic symmetry (space group Q^{224} (*Pn*3*m*)). The open aqueous nanochannels comprise a 3D labyrinthine of two intertwined networks.

Figure 1 presents models of normal (D_{Normal}) and swollen (D_{Large}) diamond-type bicontinuous cubic lattices, providing a periodic-nodal-surfaces presentation of the lipid bilayer. These two models show ideal views of the BCPs, which may form upon self-assembly of a nonlamellar amphiphile in excess aqueous phase in the absence (a) or in the presence (b) of a nanochannel-hydration enhancer. The two intertwined water-channel networks are separated by a lipid bilayer with headgroups oriented toward the aqueous phase in each supramolecular organization (for molecular presentation of the nanochannels cross-section see Figure 5 below).

The fundamental question, which motivated the present study, is the absence of proof in the literature for the stability and reversibility of the D_{Large} phase characterized by large water channels. An explanation of the mechanism of the structural transition to a D_{Large} structure is also lacking. A recent study[20a] revealed that a similar highly hydrated form of BCP can appear from a disordered sponge structure and discussed its link to the membrane fusion intermediates in biological systems.

Here the mesoscopic structures of normal and water-swollen diamond cubic phases are investigated by small-angle neutron (SANS) and synchrotron X-ray (SAXS) scattering toward more in-depth understanding of their organization and eventual inherent coexistence with other (for instance, microemulsions[43]) phases upon application of thermal and chemical (hydration) stimuli. The paper presents systematic experimental records on the stability and reversibility of the D_{Large} BCP formed by MO/OG systems in excess water environment. The results suggest a mechanism for the transitions, in which D_{Large} is involved, when external stimuli are applied.

(20) (a) Conn, C. E.; Ces, O.; Mulet, X.; Finet, S.; Winter, R.; Seddon, J. M.; Templer, R. H. *Phys. Rev. Lett.* **2006**, *96*, 108102. (b) Squires, A. M.; Templer, R. H.; Seddon, J. M.; Woenckhaus, J.; Winter, R.; Finet, S.; Theyencheri, N. *Langmuir* **2002**, *18*, 7384−7392.
(21) (a) Harper, P. E.; Gruner, S. M. *Eur. Phys. J. E.* **2000**, *2*, 217−228. (b) Harper, P. E.; Gruner, S. M.; Lewis, R. N. A. H.; McElhaney, R. N. *Eur. Phys. J. E.* **2000**, *2*, 229−245.
(22) (a) Garstecki, P.; Holyst, R. *Langmuir* **2002**, *18*, 2519−2528. (b) Garstecki, P.; Holyst, R. *Langmuir* **2002**, *18*, 2529−2537.
(23) (a) Czeslik, C.; Winter, R.; Rapp, G.; Bartels, K. *Biophys. J.* **1995**, *68*, 1423−1429. (b) Funari, S. S.; Rapp, G. *Proc. Natl. Acad. Sci. U.S.A.* **1999**, *96*, 7756−7759.
(24) (a) Nakano, M.; Sugita, A.; Matsuoka, H.; Handa, T. *Langmuir* **2001**, *17*, 3917−3922. (b) Rosa, M.; Infante, M. R.; Miguel, M. G., Lindman, B. *Langmuir* **2006**, *22*, 5588−5596.
(25) (a) Angelov, B.; Angelova, A.; Ollivon, M.; Bourgaux, C.; Campitelli, A. *J. Am. Chem. Soc.* **2003**, *125*, 7188−7189. (b) Angelov, B.; Angelova, A., Papahadjopoulos-Sternberg, B.; Lesieur, S.; Sadoc, J.-F.; Ollivon, M.; Couvreur, P. *J. Am. Chem. Soc.* **2006**, *128*, 5813−5817.
(26) Rangelov S.; Almgren, M. *J. Phys. Chem. B* **2005**, *109*, 3921−3929.
(27) (a) Spicer, P. T. *Curr. Opin. Colloid Interface Sci.* **2005**, *10*, 274−279. (b) Spicer, P. In *Marcel Dekker Encyclopedia of Nanoscience and Nanotechnology*; Schwarz, J. A., Contescu, C., Putyera, K., Eds.; Marcel Dekker: New York, 2003; pp 881−892. (c) Spicer, P. T.; Hayden, K. L.; Lynch, M. L.; Ofori-Boateng, A.; Burns, J. L. *Langmuir* **2001**, *17*, 5748−5756.
(28) (a) Siekman, B.; Bunjes, H.; Koch, M. H. J.; Westesen, K. *Int. J. Pharm.* **2002**, *244*, 33−43. (b) Kaasgaard, T.; Drummond, C. J. *Phys. Chem. Chem. Phys.* **2006**, *8*, 4957−4975.
(29) (a) Barauskas, J.; Johnsson, M.; Tiberg, F. *Nano. Lett.* **2005**, *5*, 1615−1619. (b) Barauskas, J.; Johnsson, M.; Joabsson, F.; Tiberg, F. *Langmuir* **2005**, *21*, 2569−2577.
(30) Lynch, M. L.; Ofori-Boateng, A.; Hippe, A.; Kochvar, K.; Spicer, P. T. *J. Colloid Interface Sci.* **2003**, *260*, 404−413.
(31) (a) Sagalowicz, L.; Leser, M. E.; Watzke, H. J.; Michel, M. *Trends Food Sci. Technol.* **2006**, *17*, 204−217. (b) Sagalowicz, L.; Mezzenga, R.; Leser, M. E. *Curr. Opin. Colloid Interface Sci.* **2006**, *11*, 224−229.
(32) Kraineva, J.; Nicolini, C.; Thiyaragarajan, P.; Kondrashkina, E.; Winter, R. *Biochim. Biophys. Acta* **2006**, *1764*, 423−433.
(33) (a) Angelova, A.; Angelov, B.; Papahadjopoulos-Sternberg, B.; Ollivon, M.; Bourgaux, C. *Langmuir* **2005**, *21*, 4138−4143. (b) Angelova, A.; Angelov, B.; Papahadjopoulos-Sternberg, B.; Ollivon, M.; Bourgaux, C.; *J. Drug Delivery Sci. Technol.* **2005**, *15*, 108−112. (c) Angelova, A.; Ollivon, M.; Campitelli, A.; Bourgaux, C. *Langmuir* **2003**, *19*, 6928−6935. (d) Angelova, A.; Angelov, B.; Papahadjopoulos-Sternberg, B.; Bourgaux, C.; Couvreur, P. *J. Phys. Chem. B* **2005**, *109*, 3089−3093. (e) Angelov, B.; Ollivon, M.; Angelova, A *Langmuir* **1999**, *15*, 8225−8234.
(34) Caboi, F.; Amico, G. S.; Pitzalis, P.; Monduzzi, M.; Larsson, K. *Chem. Phys. Lipids* **2001**, *109*, 47−62.
(35) (a) Shah, J.; Sadhale, Y.; Chilikuri, D. M. *Adv. Drug Delivery Rev.* **2001**, *47*, 229−250. (b) Drummond, C. J.; Fong, C. *Curr. Opin. Colloid Interface Sci.* **2000**, *4*, 449−456.
(36) (a) Keller, S. L.; Gruner, S. M.; Gawrisch, K. *Biochim. Biophys. Acta* **1996**, *1278*, 241−246. (b) Angelova, A.; Ianev, R.; Koch, M. H. J.; Rapp, G. *Arch. Biochem. Biophys.* **2000**, *378*, 93−106.
(37) (a) Puvvada, S.; Qadri, S. B.; Naciri, J.; Ratna, B. *J. Phys. Chem.* **1993**, *97*, 11103−11107. (b) Lyons, D. L.; Harman, L. P.; Morris, M. A. *J. Mater. Chem.* **2004**, 1976−1981.
(38) (a) Zhang, F.; Meng, Y.; Gu, D.; Yan, Y.; Yu, C.; Tu, B.; Zhao, D. *J. Am. Chem. Soc.* **2005**, *127*, 13508−13509. (b) Liu, T.; Wan, Q.; Xie, Y.; Burger, C.; Liu, L.-Z.; Chu, B. *J. Am. Chem. Soc.* **2001**, *123*, 10966−10972.
(39) (a) Yang, D.; O'Brien, D. F.; Marder, S. R. *J. Am. Chem. Soc.* **2002**, *124*, 13388−13389.(b) Adachi, M.; Okumura, A.; Sivaniah, E.; Hashimoto, T. *Macromolecules* **2006**, *39*, 7382−7357.
(40) Cherezov, V.; Clogston, J.; Papiz, M.Z.; Caffrey, M. *J. Mol. Biol.* **2006**, *357*, 1605−1618.
(41) (a) Razumas, V.; Talaikyte, Z.; Barauskas, J.; Miezis, Y.; Nylander, T. *Vib. Spectrosc.* **1997**, *15*, 91−101. (b) Barauskas, J.; Razumas, V.; Nylander, T. *Prog. Colloid Polym. Sci.* **2000**, *116*, 16−20.
(42) Carlsson, N.; Winge, A.-S.; Engström, S.; Åkerman, B. *J. Phys. Chem. B* **2005;** *109*, 18628−18636.
(43) (a) Teubner, M.; Strey, R. *J. Chem. Phys.* **1987**, *87*, 3195−3200. (b) Reimer, J.; Soderman, O.; Sottmann, T.; Kluge, K.; Strey, R. *Langmuir* **2003**, *19*, 10692−10702. (c) Schubert, K. V.; Strey, R.; Kline, S. R.; Kaler, E. W. *J. Chem. Phys.* **1994**, *101*, 5343−5355. (d) Hillmyer, M. A.; Maurer, W. W.; Lodge, T. P.; Bates, F. S.; Almdal, K. *J. Phys. Chem. B* **1999**, *103*, 4814−4824.

Table 1. Temperature Dependence of the Cubic Lattice Parameter, ***a***, Estimated from SAXS or SANS (at Indicated Temperatures) Patterns of Self-Assembly MO/OG Systems Generated in Excess Phosphate Buffer Medium

sample	temp (°C)	space group	lattice ***a*** (nm)	bilayer thickness (L)/ water channel D_w (nm)[a]
MO	20	*Pn*3*m*	10.36	3.3/4.0
	25	*Pn*3*m*	10.37	3.3/4.0
	30	*Pn*3*m*	10.27	3.3/3.9
	40	*Pn*3*m*	9.19	3.1/3.4
	50	*Pn*3*m*	8.55	3.1/3.0
	60	*Pn*3*m*	8.11	3.1/2.6
	65	*Pn*3*m*	7.94	3.2/2.4
	62 (ref 44)	*Pn*3*m*	8.04	3.2/2.5
MO/OG 90:10	20	*Pn*3*m* (D_{Large})	15.27	3.5/7.3
	20 SANS	*Pn*3*m* (D_{Large})	15.95	
	25 (ref 25a)	*Pn*3*m* (D_{Large})	15.05	3.5/7.1
	30	*Pn*3*m* (D_{Large})	14.75	3.5/6.9
	30 SANS	*Pn*3*m* (D_{Large})	15.83	
	40	*Pn*3*m*	12.85	3.4/5.7
	40 SANS	*Pn*3*m*	11.10	
	50	*Pn*3*m*	9.99	3.3/3.8
	60	*Pn*3*m*	9.25	3.2/3.4
	65	*Pn*3*m*	8.97	3.2/3.1
MO/OG 95:5	25	*Pn*3*m*	12.55	3.4/5.5
MO/OG 85:15	40 SANS	*Pn*3*m* (D_{Large})	14.28	
	50 SANS	*Pn*3*m*	12.08	

[a] The lipid bilayer thickness, L, and the diameter of the aqueous nanochannels, D_w, are estimated from fitting of the experimental SAXS intensities. The accuracy is ±0.2 nm.

Results

Thermo-Structural Behavior of a D_{Large} Bicontinuous Cubic Phase at Full Hydration. The performed time-resolved SAXS study characterized the modulation of the nanochannel hydration in the self-assembly amphiphilic cubic phases as a function of temperature (for SAXS details see the Supporting Information [SI]). It determined the temperature-induced changes in the diameter of the aqueous channels, D_w, and the lipid bilayer thickness, L, at three molar ratios between the amphiphilic components, namely MO/OG = 95:5, 90:10, and 85:15 (mol/mol). Table 1 summarizes the temperature dependence of the structural properties, which were revealed using the Garstecki−Holyst (GH) analytical model[22] for fitting of experimental SAXS patterns. The cubic lattice parameter, ***a***, of the D_{Large} phase displays maximum values at $T \leq 30$ °C. The value of D_w equal to 7.3 nm at 20 °C indicates that the incorporation of OG molecules brings a lot of hydration water in the network of nanochannels of the diamond-type MO cubic phase. For comparison, the BCP of pure MO displays, at full hydration, a continuous tuning of its aqueous nanochannels diameter, D_w, from 4.0 to 2.4 nm induced by thermal stimuli in the range from 20 °C to 65 °C. At variance to the nanochannel diameter (D_w), the lipid bilayer thickness, L, does not follow a monotonic decrease with temperature. Table 1 demonstrates the full agreement of our results with the MO bilayer thickness value $L = 3.2$ nm estimated by alternative techniques[44] for such a system at $T =$ 62 °C.

In *SANS* studies, hydrated self-assemblies of pure MO and of binary MO/OG mixtures (95:5, 90:10, and 85:15 mol/mol) were subjected to thermal stimulus in the range from 15 °C to 65 °C (in steps of 5 °C), followed by cooling down to the initial state. Figure 2 shows SANS results corresponding to selected levels of nanochannels hydration as controlled by the concentration of the hydration enhancer and temperature. The intense SANS correlation peak appears to be a diffraction peak matching the first-order SAXS reflections of the BCP. A less pronounced second diffraction peak was observed under conditions where the applied stimuli were able to induce the formation of a coexisting lamellar domain (see SI for 1D and 2D presentation of the SANS intensities and a description of the patterns of the liquid crystalline phases).

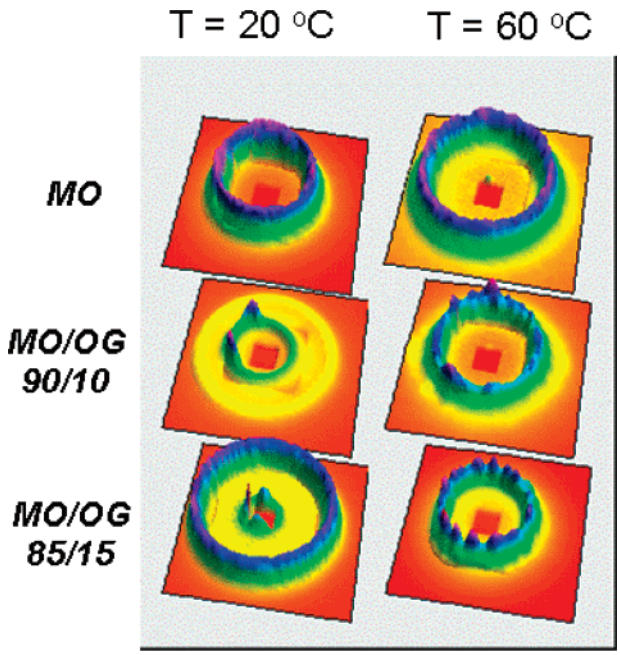

Figure 2. Small-angle neutron scattering (SANS) patterns of self-assembly MO/OG systems with molar ratios MO/OG 100:0, 90:10, and 85:15 (mol/mol) corresponding to selected stages of the nanochannels hydration at $T = 20$ °C (left column) and at $T = 60$ °C (right column) from the thermal scan performed between 15 °C and 65 °C under excess water conditions. The q-range is from −0.24 to 0.24 ($Å^{-1}$).

Effect of the Molar Composition. At a molar ratio of 90:10 MO/OG and $T < 30$ °C, the cubic lattice parameter, ***a***, of the self-assembly phase is nearly 50% greater (a D_{Large} cubic phase) than that of the D_{Normal} cubic structure. At $T \geq 40$ °C, the D_{Large} cubic structure begins to transform into a D_{Normal} one, owing to dehydration of the nanochannels. This is associated with an essential decrease in the lattice spacing, ***a***, and in the water channel diameter, D_w (Table 1). The lipid bilayer thickness, L, in the MO/OG 90:10 cubic assembly also decreases with the rise in temperature, which correlates with an increase in the interfacial curvature and squeezing out of OG molecules from the bilayer.

The 2D SANS patterns of this system are characterized by pronounced spots in the azimuthal intensities at $T \geq 40$ °C (see Figure 2 ($T = 60$ °C) and Figure 3S). Spot reflections are indicative for the formation of large liquid-crystalline domains of single-crystal cubic nature. Thus, the applied temperature stimulus triggers the arbitrarily oriented D_{Large} "polycrystalline" domains to convert into growing spontaneously oriented D_{Normal} domains. This structural transition of the soft-matter assembly, related to the dehydration of nanochannels, does not change

(44) (a) Marrink, S.-J.; Tieleman, D. P. *J. Am. Chem. Soc.* **2001**, *123*, 12383−12391 (b) Qui, H.; Caffrey, M. *Biomaterials* **2000**, *21*, 223−234.

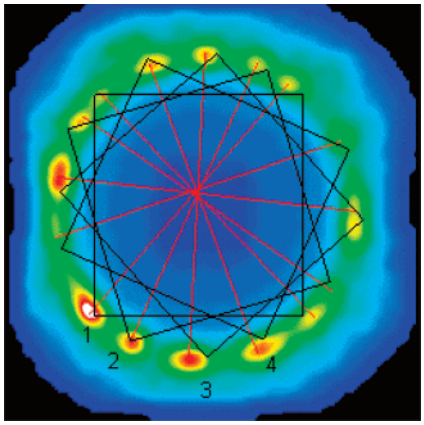

Figure 3. Two-dimensional SANS image recorded with a self-assembly MO/OG 85/15 (mol/mol) cubic system at 60 °C. The observed reflection spots characterize the supramolecular architecture of a D_{Normal} bicontinuous cubic phase formed upon temperature-induced dehydration of the aqueous nanochannels of a D_{Large} swollen cubic phase. The individual diffraction spots represent cubic domain sizes larger than the beam size. These spots are grouped on the apexes of four identical squares (denoted as 1, 2, 3, and 4). In the reciprocal space, they represent the *110*, *$^{-}$110*, *1^{-}10*, and *$^{-}$1^{-}10* indexes corresponding to the first allowed reflection of single-crystal *Pn*3*m* cubic domains.

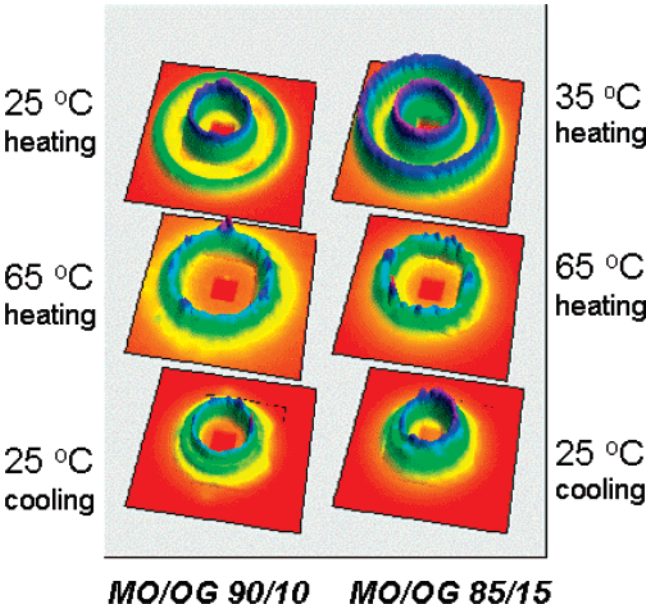

Figure 4. SANS patterns demonstrating the structural transition from a D_{Large} to a D_{Normal} cubic structure on heating from $T = 25$ °C to $T = 65$ °C in MO/OG 90:10 (mol/mol) system (left column) and from $T = 35$ °C to $T = 65$ °C in MO/OG 85:15 (mol/mol) system (right column). With both amphiphilic compositions, cooling from 65 °C to 25 °C reveals the reversibility of the D_{Large} phase and the irreversibility of the lamellar peak at $q \approx 0.12$ (Å^{-1}). Only the D_{Large} peak at $q \approx 0.05$ (Å^{-1}) is recovered upon cooling back to $T = 25$ °C. The q-range is from -0.24 to 0.24 (Å^{-1}).

the fluid LC state of the bicontinuous lipid bilayer. The recording of individual diffraction spots for a lyotropic cubic phase comes from the fact that the growing cubic domains have a larger size compared to the beam spot size.

Increasing the OG concentration, to yield a total molar ratio MO/OG 85:15 (mol/mol), causes a shift in the phase transition temperature from a lamellar to a cubic phase state. A lamellar phase is dominant at MO/OG 85:15 molar ratio at temperatures between 15 and 30 °C (see Figure 2 ($T = 20$ °C) and Figure 4S). Under these conditions, lipid domains rich with OG adopt a lamellar structure owing to the induced decrease in the monolayer curvature.[33e] The repeat bilayer spacing of the lamellar phase is determined to be $\boldsymbol{d} = 4.91$ nm. Upon an increase in the temperature the lamellar domain coexists with a growing cubic phase domain. A D_{Large} phase is promoted at $T = 35$ °C, and it becomes the major phase at $T = 40$ °C, displaying a homogeneous 2D SANS pattern (without pronounced spots). At 40 °C, the D_{Large} cubic lattice unit is maximum, $\boldsymbol{a} = 14.28$ nm. This $\boldsymbol{a}$ value is approximately equal to that of the D_{Large} phase formed in the MO/OG 90:10 system at around 35 °C. Perhaps it corresponds to the maximum swelling degree that could be achieved in BCP self-assembled at the investigated amphiphilic compositions.

Indexing in the Reciprocal Space. Figure 3 analyzes the 2D SANS pattern of the MO/OG 85:15 sample recorded at 60 °C. We identified reflections belonging to the same indexing in the reciprocal lattice. The allowed first diffraction peak for the *Pn*3*m* cubic symmetry corresponds to Miller indices *110*, *$^{-}$110*, *1^{-}10*, and *$^{-}$1^{-}10*. The cubic lattice vectors are orthogonal and of equal length. The projection of a face of the cube can be a square in the reciprocal space, depending on the sample orientation with respect to the incident beam. This appears to be the case shown in Figure 3: the spots, indexed as *110*, *$^{-}$110*, *1^{-}10*, and *$^{-}$1^{-}10*, constitute the apexes of a square. This indicates that the *a*, *b*, and *c* axes of the cubic lattice are parallel to the incident beam, thus yielding the observed square projections in the reciprocal space. By applying azimuthal rotation of the square around the incident beam direction, we identified the existence of at least four orientations of cubic domains in the investigated complex fluid sample present in the beam (see the four squares in Figure 3). Probably many more cubic domains could be identified if the measurement cell could be rotated with respect to the beam direction.

Reversibility of the $D_{Large} \rightarrow D_{Normal}$ Structural Transition. The SANS patterns in Figure 4 indicate that the D_{Large} cubic structure is reversible in thermal cycles with MO/OG systems of both 90:10 and 85:15 molar ratios. Starting from a D_{Large} phase characterized by a mosaic spread of cubosomic domains at low temperatures ($T < 25$ °C for the MO/OG 90:10 system or $T < 35$ °C for the MO/OG 85:15 system), one establishes that the cubosomic domains become correlated upon heating to 65 °C. They stack into growing single-crystal domains as revealed by the pronounced spots on the circular SANS patterns. Upon cooling down to 25 °C, the diffraction peak of the D_{Large} phase is recovered ($q \approx 0.06$ Å^{-1}). This means that the nanochannels of the D_{Large} phase reversibly swell upon cooling in the presence of the hydration enhancer OG that acts as an interfacial curvature modulator. The D_{Large} cubic phase forms as a reversible phase relatively quickly (within few hours).

At variance to the relatively rapid kinetics of the cubic $D_{Normal} \rightarrow D_{Large}$ structural transition (time scale of the order of hours), the kinetics of nucleation and growth of lamellar domains upon temperature quenching down to 25 °C is rather slow (more than 1 day), thus preventing the reversibility of the lamellar domain in thermal cycles. Indeed, the lamellar peak at $q \approx 0.12$ Å^{-1} is not recovered during the cooling scan to 25 °C (see the bottom patterns at 25 °C in Figure 4 which are not identical to those in the heating scan at 25 °C, where the lamellar domain coexists with a cubic phase). The D_{Large} cubic phase was found to coexist with lamellar domains exclusively when the samples were stored for prolonged equilibration time (several days) at nearly zero

temperature (i.e., under conditions favoring the formation of a lamellar L_c monoolein phase).

Discussion

The swollen cubic D_{Large} phase forms at low temperatures upon incorporation of a small molar fraction (≤10 mol%) of the amphiphilic compound OG in the fully hydrated MO cubic phase. We found that at MO/OG 80:20 molar ratio, a cubic structure could not form at temperatures below 50 °C. This means that an additive (OG) molar fraction higher than 15 mol % will destabilize the D_{Large} cubic phase at low and body temperatures due to the OG effect on the interfacial monolayer curvature,[33e] favoring the formation of a lamellar supramolecular assembly at such compositions.

Mechanism of the $D_{Large} \rightarrow D_{Normal}$ Transition Associated with Nanochannel Dehydration, Domain Alignment, and Curvature-Induced Molecular Demixing. The SANS study established spontaneous orientation of single-crystal domains only in the self-assembled MO/OG systems (Figures 2 and 4) but not in the pure MO/water cubic system, which lacks a hydration-modulating agent. The spontaneous orientation of single-crystal domains, under the applied temperature and hydration stimuli, appears to be a feature of the MO/OG BCP, provided that no shearing is applied in the present experiments for alignment of the sample. The orientation seems to be caused by the nanofluidic flow related to the diffusion of the guest agent (OG) from the interior to the exterior of the bicontinuous bilayer structure at temperatures above the $D_{Large} \rightarrow D_{Normal}$ transition temperature. Generally, the inherent 3D connectivity of the BCP does not imply domain alignment[7] (Figure 2). However, with nanoparticulate systems, an external stimulus has been needed to achieve highly ordered small-scale assemblies. Studies on cubosomes[12b,29] have shown that glyceryl monooleate nanoparticles develop single-crystal internal structures at rather high temperatures ($T \approx 125$ °C). Anchoring effects on the walls of the measurement cell could induce spontaneous domain orientation as well.

Thermal stimuli on cooling can lead to quenching of the spontaneously oriented domain organization. The spots of the crystalline domains in the SANS patterns (Figure 4) disappeared after cooling back to 25 °C. Therefore, single-crystal orientation is not preserved upon cooling down. These orientation−disorientation processes may be related not only to the high temperature and higher OG concentration stimuli that provoke the spontaneous domain alignment but also to the presence of two water-channel networks in the supramolecular double diamond-type cubic structure.[15,17,25b] One of these networks (Figure 1) is open to the excess water, while the other can be closed. It may be expected that the hydration/dehydration processes occur via asymmetry in the two water-channel networks. Nevertheless, the established reversibility of the D_{Large} BCP confirms the structural stability of the water-swollen nanostructures at ambient temperatures.

It could be suggested that phase separation between the components at elevated temperatures associated with the growth of D_{Normal} cubic domains. The increase in temperature causes a respective increase in the interfacial monolayer curvature of the amphiphilic MO/OG bilayer. This might induce progressive expelling of the guest OG molecules from the lipid bilayer plane. Figure 5 presents the suggested molecular mechanism of the

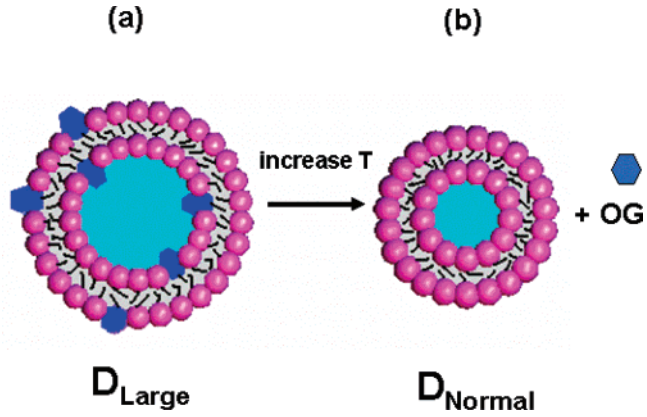

Figure 5. Proposed molecular mechanism of the transition cubic $D_{Large} \rightarrow$ cubic D_{Normal}. (a) Cross section of a weakly curved MO/OG bilayer in a D_{Large} cubic structure. (b) Cross section of a highly curved MO bilayer in a D_{Normal} cubic structure. The temperature-induced increase in the interfacial monolayer curvature is suggested to lead to squeezing out the OG molecules from the lipid bilayer and their release toward the aqueous environment.

nanochannel dehydration accompanying the $D_{Large} \rightarrow D_{Normal}$ structural transition. In this mechanism, the temperature increase causes an increase in the monolayer curvature upon nanochannel dehydration in self-assembled cubic MO/OG systems. This results in the squeezing out of the OG molecules from the lipid bilayer of the D_{Large} structure (a) to the aqueous phase on the occasion of its transition to a D_{Normal} structure (b).

Several arguments are in favor of the squeezing-out concept for OG release from the lipid bilayer. (i) The established orientation and correlation into single-crystal domains would not occur if the guest OG molecules were not expelled from the supramolecular structure toward the aqueous environment at higher temperatures. (ii) The bilayer thickness becomes smaller on heating, which suggests that the guest OG molecules are likely squeezed out of the bilayer to the aqueous phase when the lipid monolayer curvature increases. (iii) The obtained results (Table 1) for the cubic lattice spacing, ***a***, of MO/OG cubic phases at higher temperatures are very close to the lattice spacing of the pure MO cubic phase. Therefore, OG should be released from the supramolecular structure.

Regarding the mechanism of the release of encapsulated guest (globular protein) molecules upon increasing temperature, we suggest that the protein should be released outside the cubosomic assembly since the cubic lattice parameter determined at temperature above 50 °C approaches that of pure monoolein, which lacks encapsulated guest protein. Respectively, the nanochannel diameters decrease with rising temperature. At higher temperatures, the system starts to orient into single-crystal domains (Figure 3). This suggests that the guest molecules are squeezed out from the cubosomic building blocks.

Perspectives for Drug Delivery Applications of Stimuli-Responsive BCP. While taking advantage of nanoscale bicontinuous LC systems for encapsulation of proteins and peptide drugs, an important question is the stability of the resulting self-assembled structures at low temperatures, ∼4 °C (conditions employed for storage of several biopharmaceuticals). The new water-swollen (D_{Large}) BCP appears to be attractive for development of nanoscale drug delivery systems as it forms at temperatures below 45 °C and it remains stable down to 0 °C. Furthermore, we found that it is a stable and a reversible phase. OG was studied here as a model amphiphilic molecule serving

as a hydration enhancer of the aqueous nanochannels. In drug delivery applications, this hydration-modulating agent could be substituted by other injectable surfactants (e.g., polysorbate 80) or by some amphiphilic drugs (e.g., miltefosine) provided that these guest molecules could show a capacity to increase the hydration of the nanochannels. On their own, proteins (transferrin, immunoglobulin, and others) may influence the hydration of the cubic lipid systems[33b,c] as well.

The fundamental result that the hydration of the aqueous channels of the MO cubosomic carrier is stimulus (chemical and temperature) sensitive and that the structural $D_{Large} \rightarrow D_{Normal}$ transformation occurs at approximately physiological temperatures could be explored in pharmaceutical perspectives by putting forward stimuli-responsive local delivery mechanisms. Taking into account that several pathology processes are accompanied with local temperature increases (by 2−5 °C) in diverse tissues and organs, one could suggest that the structural transitions observed at temperatures above 35 °C could be explored toward stimuli-sensitive delivery strategies. Upon administration in vivo at 37 °C (or at a higher temperature in case of a pathological event) the cubosomic carrier will fall into a structural transformation accompanied by an increase in the curvature of the lipid monolayer, induction of local phase separation of the amphiphilic components, and release (squeeze out) of the guest compound outside the lipid nanovehicle. Thus, the local release of encapsulated guest molecules will be triggered by the temperature change. This concept hypothesizes a stimuli-sensitive mechanism of delivery from a cubosomic nanocarrier.

Conclusion

The functionalization of the lipid bilayer by a proper water-soluble amphiphile (OG in this work) provides a facile means to control the hydration of the water nanochannels, specifically their diameters and capacity to encapsulate guest biomolecules (for instance globular proteins or peptides). The concentration of OG is an important parameter permitting control of the temperature of the $D_{Large} \rightarrow D_{Normal}$ structural transformation. The obtained results suggest that ∼5−10 mol % OG would be sufficient to swell the cubic nanochannel network to incorporate soluble proteins. As the stability of the 3D mesoscale amphiphilic structure is crucial for its potential applications in drug delivery systems, it is essential to emphasize that it can stably persist upon storage during several months by preserving its large aqueous nanochannels. Here we established that the structural transition $D_{Large} \rightarrow D_{Normal}$ is reversible with regards to thermal stimuli in the presence of the hydration and interfacial-curvature modulator OG. A thermo-response mechanism is suggested for the release of entrapped molecules.

Acknowledgment. The NMI3 research project has been supported by the European Commission under the 6th Framework Programme through the Key Action: *Strengthening the European Research Area, Research Infrastructures*. Contract no.: RII3-CT-2003-505925. The comments and suggestions of the editor and the reviewers are gratefully acknowledged. This paper is dedicated to the memory of Dr. Michel Ollivon, a Research Director at CNRS.

Supporting Information Available: Experimental section and additional results with SAXS and SANS patterns. This material is available free of charge via the Internet at http://pubs.acs.org.

JA072725+